Supplementary information for "Design of simple interactions to assemble complex crystals from binary mixtures of colloidal particles"

Beth Hsiao-Yen Wei,[1, a)] C. Levi Petix,[2, a)] Qizan Chen,[1] Michael P. Howard,[2, b)] and Jeetain Mittal[1, 3, 4, c)]

[1)] *Artie McFerrin Department of Chemical Engineering, Texas A&M University, College Station*

[2)] *Department of Chemical Engineering, Auburn University, Auburn, AL 36849, USA*

[3)] *Department of Chemistry, Texas A&M University, College Station*

[4)] *Interdisciplinary Graduate Program in Genetics and Genomics, Texas A&M University, College Station*

[a)] These authors contributed equally.

[b)] Electronic mail: mphoward@auburn.edu

[c)] Electronic mail: jeetain@tamu.edu

TABLE S1. Lattice vectors (in units of σ), fractional coordinates and types of particles in unit cell, number of unit cell repeats, and total number of particles for each target crystal structure.

	square	honeycomb	BCC	cubic diamond
lattice vectors	$(2, 0)$, $(0, 2)$	$(3, 0)$, $\left(3/2, 3\sqrt{3}/2\right)$	$\left(2/\sqrt{3}, 0, 0\right)$, $\left(0, 2/\sqrt{3}, 0\right)$, $\left(0, 0, 2/\sqrt{3}\right)$	$\left(4/\sqrt{3}, 0, 0\right)$, $\left(0, 4/\sqrt{3}, 0\right)$, $\left(0, 0, 4/\sqrt{3}\right)$
unit cell	$(0, 0, \mathrm{A})$, $(1/2, 0, \mathrm{B})$, $(0, 1/2, \mathrm{B})$, $(1/2, 1/2, \mathrm{A})$	$(0, 0, \mathrm{A})$, $(2/3, 0, \mathrm{B})$, $(0, 1/3, \mathrm{B})$, $(1/3, 1/3, \mathrm{A})$, $(1/3, 2/3, \mathrm{B})$, $(2/3, 2/3, \mathrm{A})$	$(0, 0, 0, \mathrm{A})$, $(1/2, 1/2, 1/2, \mathrm{B})$	$(0, 0, 0, \mathrm{A})$, $(1/2, 1/2, 0, \mathrm{A})$, $(1/2, 0, 1/2, \mathrm{A})$, $(0, 1/2, 1/2, \mathrm{A})$, $(1/4, 1/4, 1/4, \mathrm{B})$, $(3/4, 1/4, 3/4, \mathrm{B})$, $(3/4, 3/4, 1/4, \mathrm{B})$, $(1/4, 3/4, 3/4, \mathrm{B})$
# repeats	(16, 16)	(13, 13)	(10, 10, 10)	(5, 5, 5)
total # particles	1024	1014	2000	1000

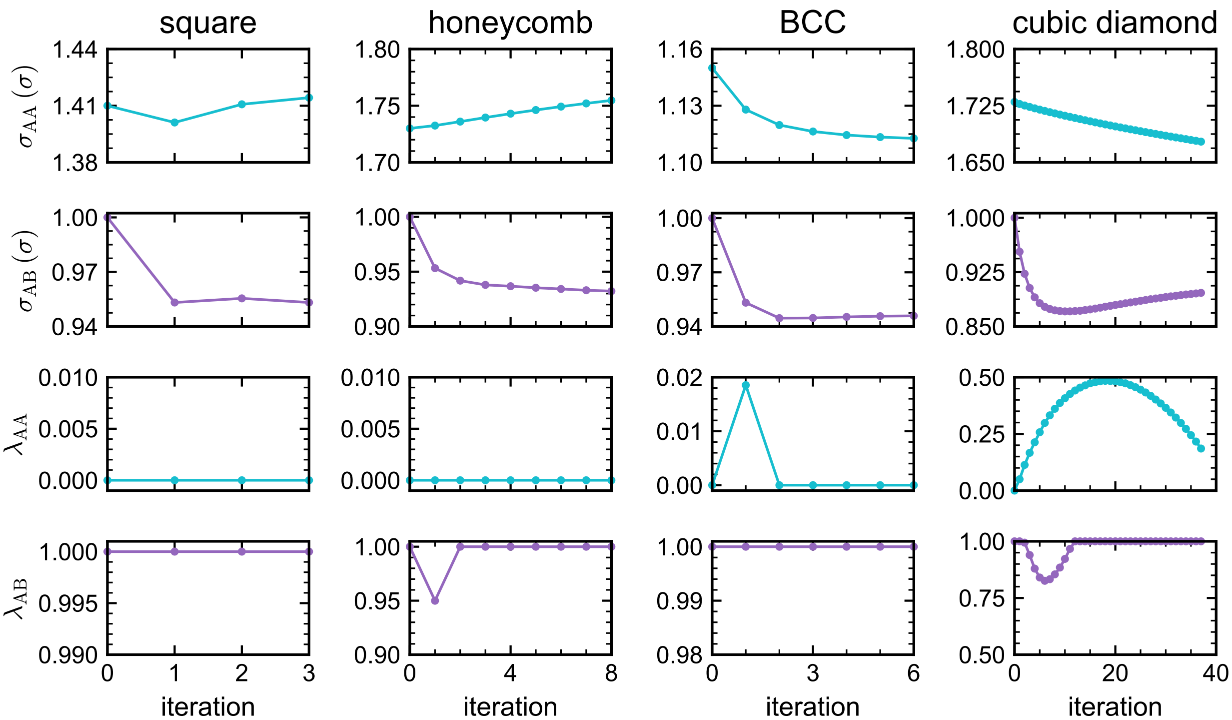

FIG. S1. Evolution of variables during optimization for square, honeycomb, BCC and cubic diamond.

TABLE S2. Iteration of optimization at which convergence was achieved and corresponding parameters for each crystal structure.

	square	honeycomb	BCC	cubic diamond
iteration	3	8	6	37
σ_{AA}	1.414	1.755	1.113	1.677
σ_{AB}	0.953	0.932	0.946	0.896
λ_{AA}	0.000	0.000	0.000	0.185
λ_{AB}	1.000	1.000	1.000	1.000

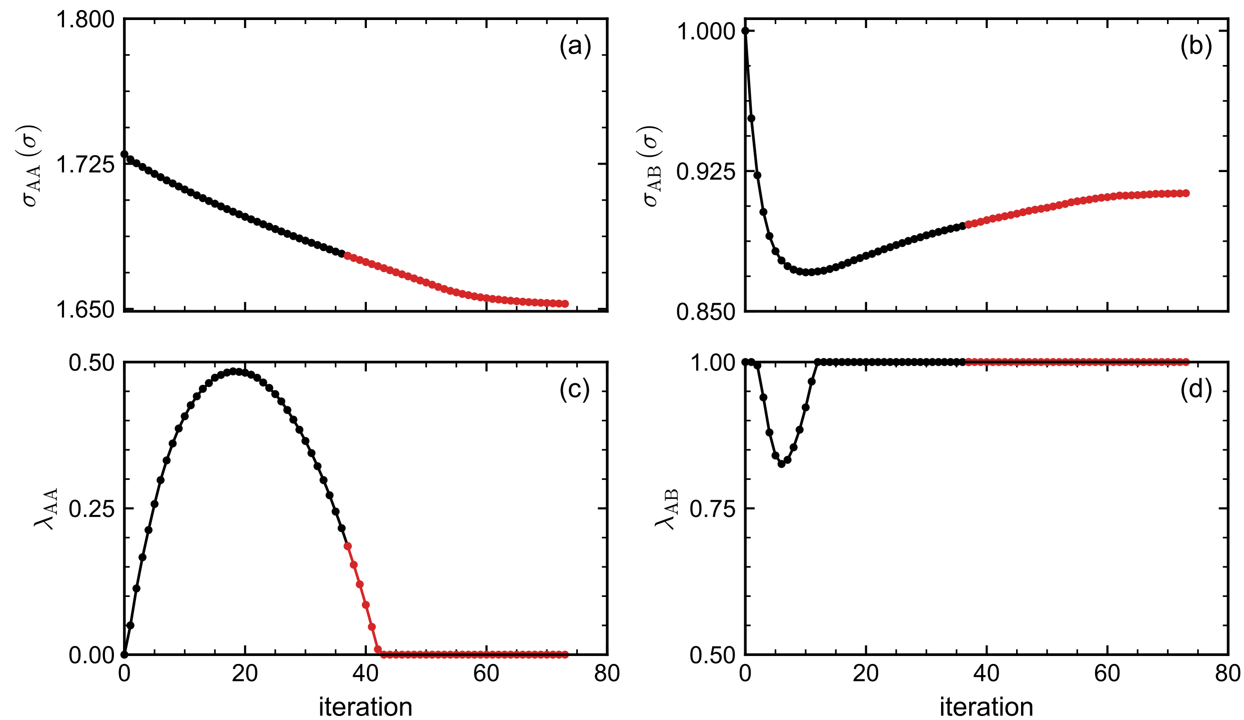

FIG. S2. Evolution of optimization parameters during inverse design for cubic diamond with original (black, convergence criterion 10^{-2}, from Fig. S1) and stricter (red, 10^{-3}) convergence criteria.

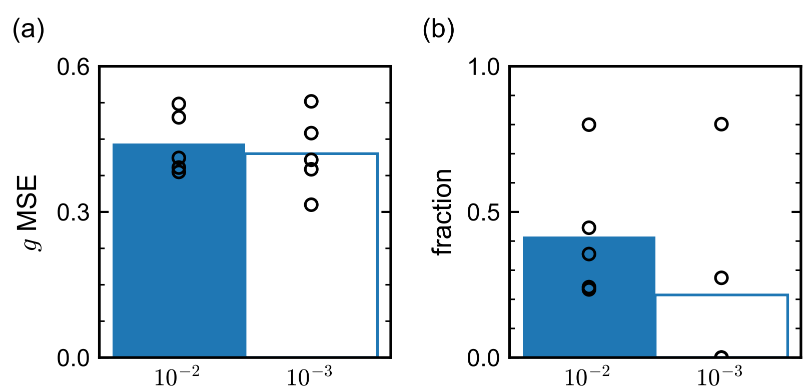

FIG. S3. Average (a) mean squared error (MSE) in type-agnostic radial distribution function g and (b) fraction of particles classified as being in target lattice for 5 independent simulations following the validation (isothermal compression) protocol using potentials obtained from the inverse-design procedure for cubic diamond with convergence criteria of 10^{-2} and 10^{-3}.

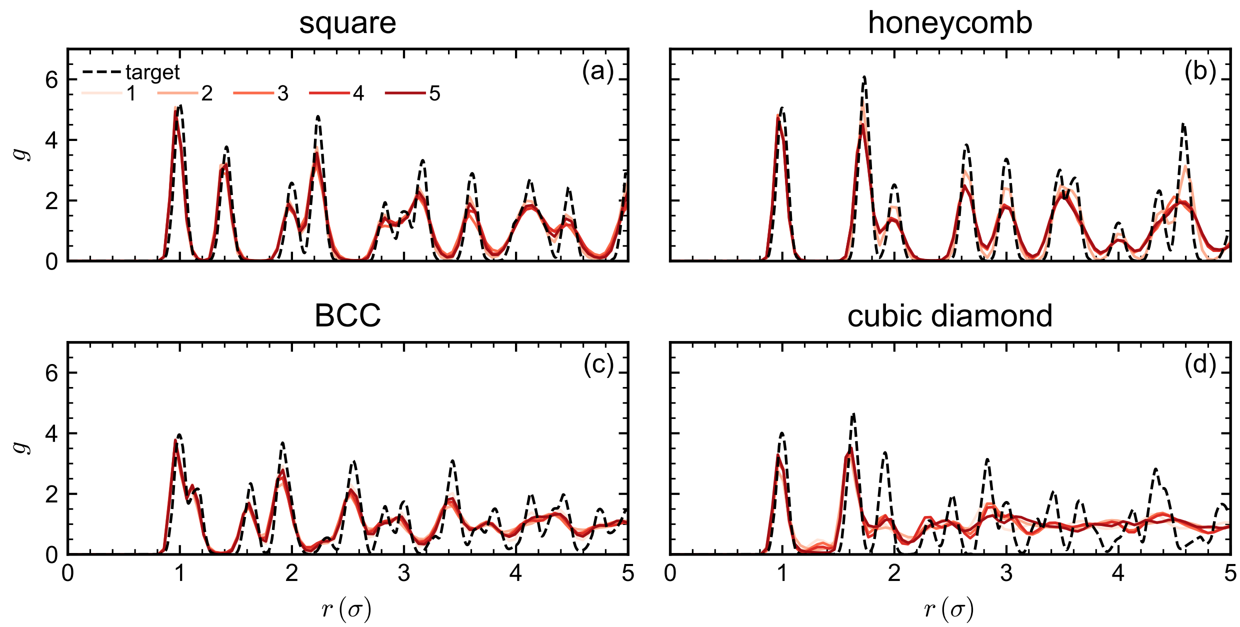

FIG. S4. Type-agnostic radial distribution function g sampled from five independent validation (isothermal compression) simulations using the potential designed during isochoric temperature cycling for (a) square (b) honeycomb (c) BCC and (d) cubic diamond.

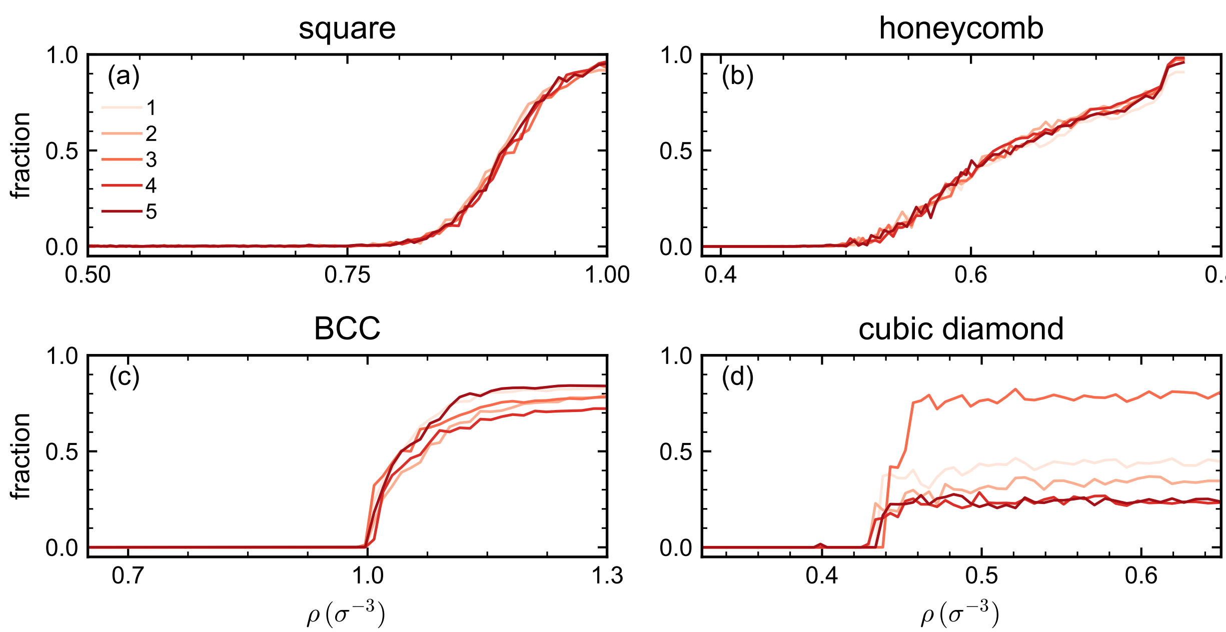

FIG. S5. Same as Fig. S4 for the fraction of particles classified as being in target lattice.

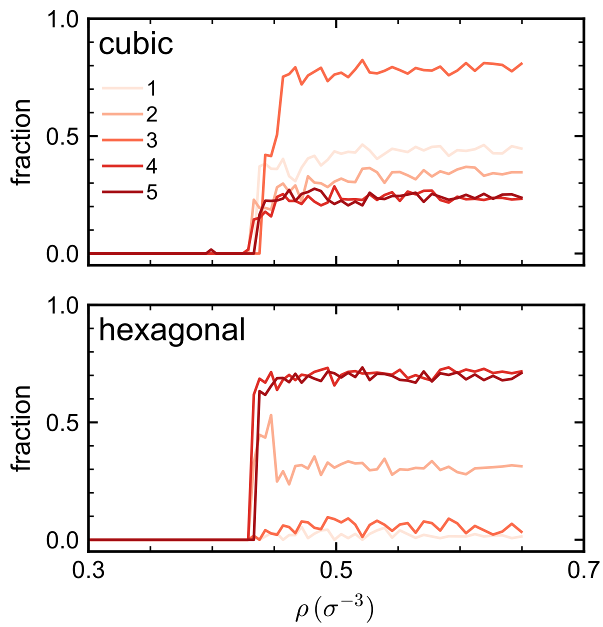

FIG. S6. Fraction of particles classified as being cubic or hexagonal diamond for the same simulations as in Figs. S4d and S5d.

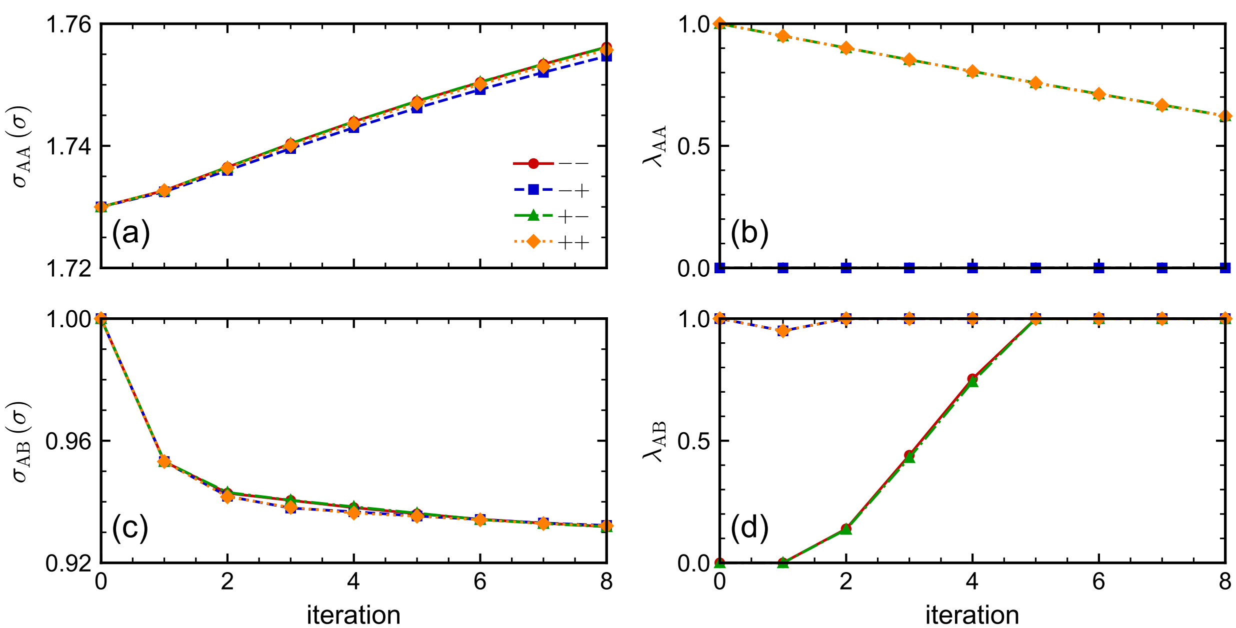

FIG. S7. Evolution of variables during optimization for honeycomb initialized from $(\lambda_{AA}, \lambda_{AB}) = (0, 0)$, $(0, 1)$, $(1, 0)$, and $(1, 1)$. The legend uses the notation from the main text, where $-$ is 0 and $+$ is 1. At convergence, the parameters for the $++$ design were $\sigma_{AA} = 1.756$, $\sigma_{AB} = 0.932$, $\lambda_{AA} = 0.622$, and $\lambda_{AB} = 1.000$.

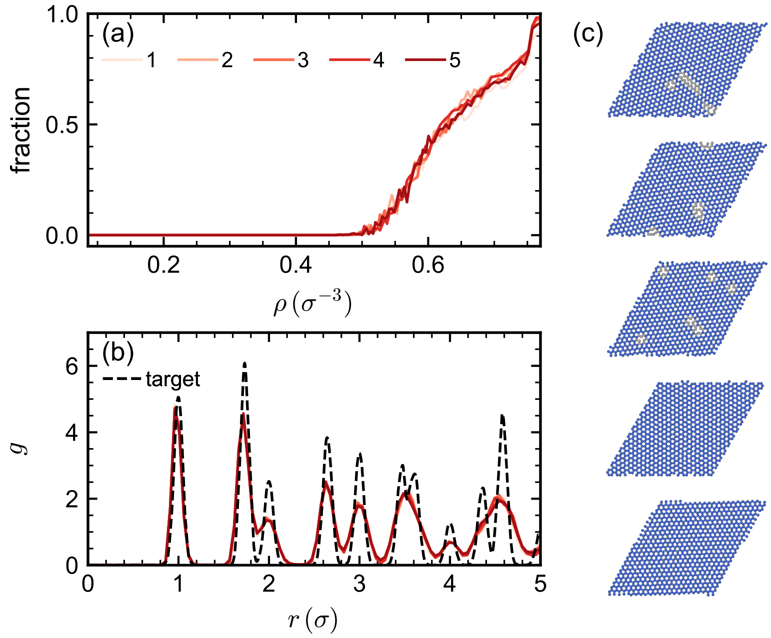

FIG. S8. Five independent validation (isothermal compression) simulations for the honeycomb ++ design. (a) Fraction of particles classified as being honeycomb. (b) Type-agnostic radial distribution function g. (c) Final particle configuration. Particles classified as honeycomb are blue, while other particles are gray.

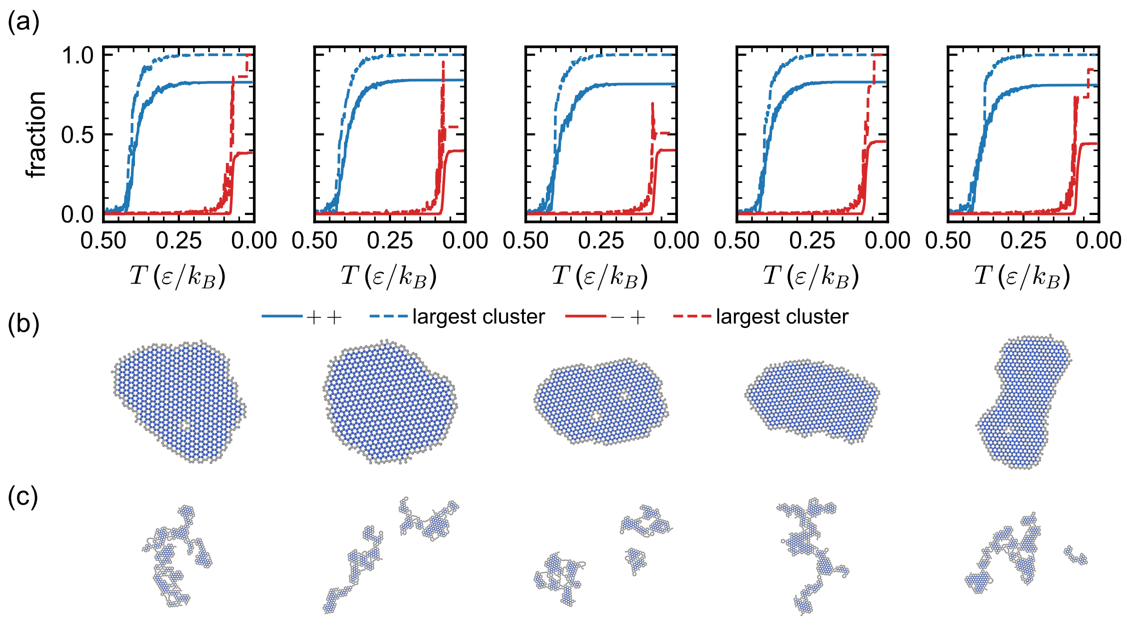

FIG. S9. Five independent dilute isochoric cooling simulations in two dimensions for the honeycomb −+ and ++ designs. (a) Fraction of particles classified as being honeycomb and being in the largest cluster. (b) Final particle configuration for the ++ design. Particles classified as honeycomb are blue, while other particles are gray. (c) Same as (b) for the −+ design.

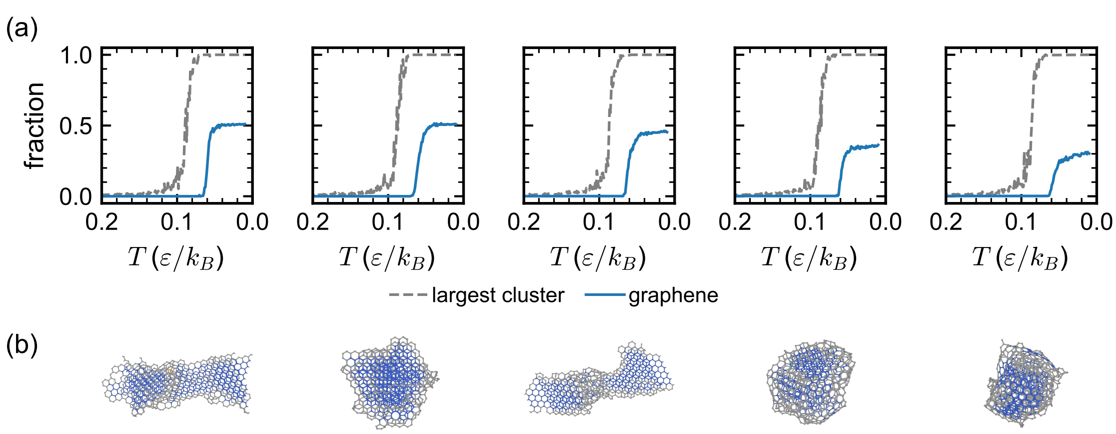

FIG. S10. Five independent dilute isochoric cooling simulations in three dimensions for the honeycomb −+ design. (a) Fraction of particles classified as being graphene and being in the largest cluster. (b) Final particle configuration. Particles classified as graphene are blue, while other particles are gray.

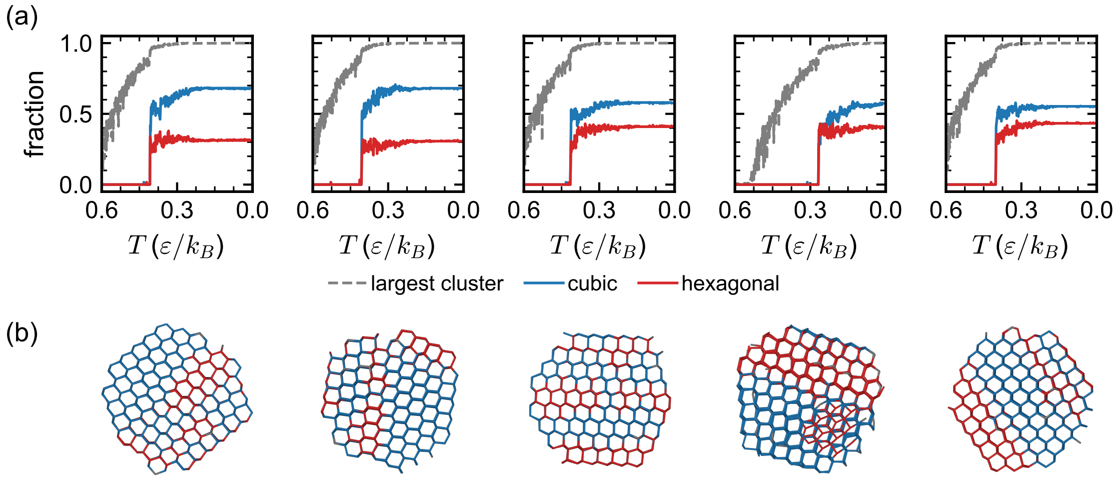

FIG. S11. Five independent dilute isochoric cooling simulations in three dimensions for the honeycomb ++ design. (a) Fraction of particles classified as being cubic or hexagonal diamond and being in the largest cluster. (b) Final particle configuration. Particles classified as cubic diamond are blue or as hexagonal diamond are red, and other particles are gray.

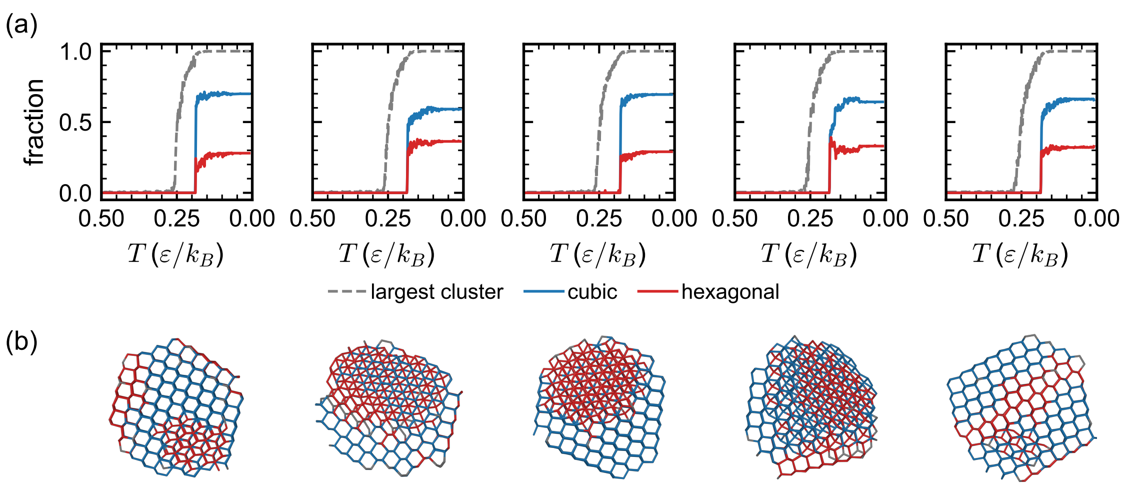

FIG. S12. Five independent dilute isochoric cooling simulations for the cubic diamond design. (a) Fraction of particles classified as being cubic and hexagonal diamond and being in the largest cluster. (b) Final particle configuration. Particles classified as cubic diamond are blue or as hexagonal diamond are red, and other particles are gray.

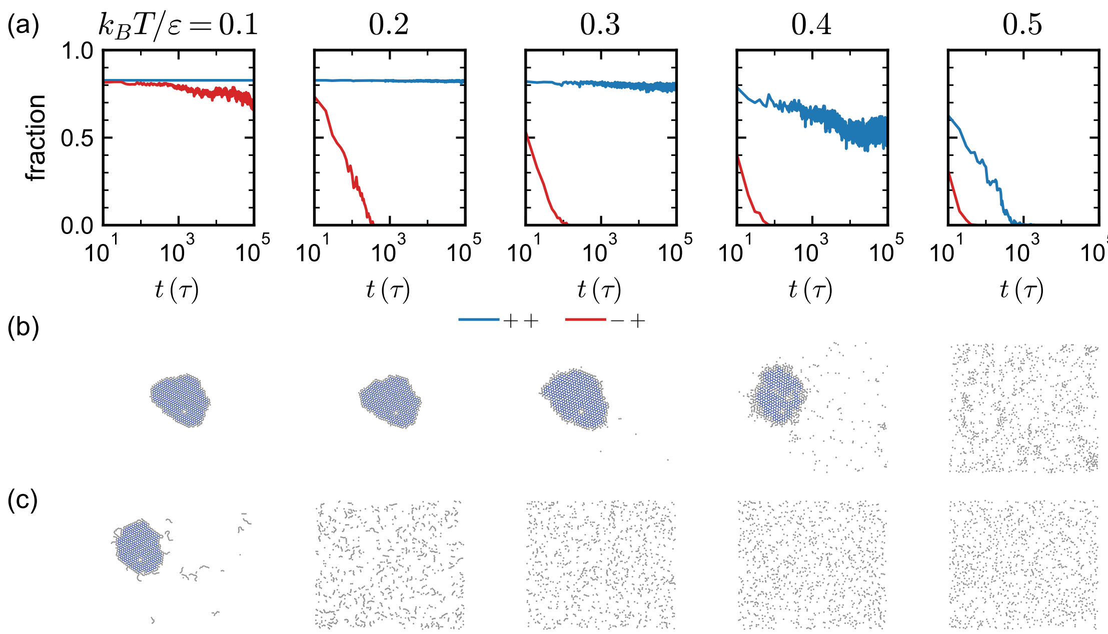

FIG. S13. Dilute isothermal–isochoric simulations initialized from the honeycomb crystallite assembled in Fig. S9b at $0.1 \leq k_BT/\varepsilon \leq 0.5$ in increments of 0.1. (a) Fraction of particles classified as honeycomb for honeycomb ++ and −+ designs. (b) Final particle configuration at each temperature for ++ design. Particles classified as honeycomb are blue, while other particles are gray. (c) Same as (b) for the −+ design.